8th EnvImeko - IMEKO TC19 Symposium on Environmental Instrumentation and Measurements
October 29-30, 2019, Sfax, Tunisias

Development of new conditioning circuit for ISFET sensor

Ahmed Gaddour [a,b], Wael Dghais [b,c], Belgacem Hamdi [b,c], Mounir Ben Ali [c,d]

[a] National Engineering School of Monastir (ENIM), University of Monastir, Monastir 5000, Tunisia.
[b] Electronics and Microelectronics Laboratory, LR99ES30, Faculty of Sciences of Monastir, University of Monastir, Monastir 5000.
[c] Higher Institute of Applied Sciences and Technology of Sousse (ISSATSo), University of Sousse, Sousse 4003, Tunisia.
[d] Nanomaterials, Microsystems for Health, Environment and Energy Laboratory, LR16CRMN01, Centre for Research on Microelectronics and Nanotechnology, Sousse 4034, Tunisia

Abstract- It is commonly known that most readout circuits of the pH-ISFET, with temperature cancelation, were designed using MOSFET working in strong regime. Nevertheless, a classes of circuits elaborated with respect to MOSFET operating in weak inversion and moderate regime are also suitable for low-power systems such as ISFET sensor array for DNA detection. In this work a new integrated interface circuit that can perform a great temperature compensation to enhance stability of the readout circuit operating in weak inversion for ISFET was developed. At first, the experimental results agree with the ISFET macro model in wide range of pH with a sensitivity about of 54mV/pH. Second, we investigated the ISFET response for a wide temperature range from -20 to 150°C. After that we propose a new conditioning circuit operating in weak inversion regime, the simulation result prove that the design technique permits to enhance the temperature insensitivity (about of 13 10^{-6}V/°C) and a power consumption in order of 49 µW.

Keys words— ISFET sensor, conditioning circuit, Temperature compensation.

I. INTRODUCTION

Chemical sensors are generally dedicated to the detection of gases ions and biological species [1]. These sensors have become indispensable today because of their many application fields. Their use in fields like biochemistry, biology, safety, medicine, agriculture and the environment has become increasingly important [2]. In the context of this work, the sensors that we used for modeling and experimental setup is constituted of sensitive layer placed in contact with a transducer which translates the chemical into electrical signal. The ISFET (Ion Sensitive Field Effect Transistor) micro-sensors using a field effect transistor as transducers are the most promising because of their high specificity in terms of sensitivity, selectivity and accuracy compared to those of other similar analytical methods [3]. This type of sensor has several considerable advantages such as low cost, the possibility of miniaturization [4], the possibility of realization of multi-sensory and especially the possibility of integrating signal conditioning electronics [5, 6]. The latter (conditioning circuit) aims to reduce the undesirable effects of the influence quantities, in particular the effect of temperature [7], which has a considerable influence on the behaviour of the chemical sensors. Bibliographic studies which are dedicated to the development of ISFET semiconductor micro-sensors showed many researches directed towards to the use of new membranes in order to improve their operating characteristics[4, 8-10]. Nevertheless, since they are sensitive to temperature and light variation the conventional method used for signal-processing of ISFET, in particular, the current-voltage conversion systems, do not reach finest performance. For these reasons, in this paper, we developed a new technique to optimize the detection abilities of the ISFET micro-sensor. For modelling and simulation, we used ADS (advanced design System) tool which is designed for the modulation of WIFI and microwave system. In our work, we oriented this simulator to biosensor associated with conditioning system.

The paper is organized as follows, section II presents the conventional ISFET macro-model. In section III we simulate the macro model under Advanced Design System (ADS). While an optimized circuit is given in section IV in which the performance of circuit is compared with other works table 3. Conclusion is drawn in Section V.

II. ISFET MACRO-MODEL

Refer to many studies made by Bergveld [11-13], we found that the ISFET and the MOSFET have similar structures, unless we use the membrane to measure the concentration of a specified ions in an electrolyte [13], due to ionic activity at the surface, between electrolyte-insulator surface the variation of the threshold voltage is proportional to the value of a pH. The insulator electrochemical properties were combined with MOSFET physics[14]. With the consideration of the threshold voltage V_{th} (ISFET) in I-V formula of the MOSFET, we can obtain static model of ISFET:

$$I_{ds} = I_0 e^{\left(\frac{V_{gs}-V_{t_I}}{\eta U_t}\right)} \quad (1)$$

where I_0 is a characteristic current, U_t is the thermal voltage and η is the slope factor of the subthreshold. This mode of operation offers the possibility to have a low power and a high voltage gain.

The ISFET threshold voltage formula include electrochemical as well as terms derived from the MOSFET [14]:

$$V_{t_I} = \left(E_{ref} + \varphi_{1j}\right) - (\varphi_0 - \chi_e) - \left[\frac{Q_{ss}+Q_{sc}}{C_{ox}} - 2\varphi_f + \frac{\varphi_{sc}}{q}\right]$$

$$= V_{t_M} + E_{ref} + \varphi_{lj} + \chi_e - \varphi_0 - \frac{\varphi_m}{q} \quad (2)$$

Where, V_{t_M} is the threshold voltage of the MOSFET transistor, φ_{lj} is the liquid-junction potential drop between the electrolyte and the reference, φ_0 is the voltage of the electrolyte–insulator interface that determines the sensitivity of the ISFI (3) I^+ concentration, χ_e is the electrolyte–insulator surface dipole voltage, q charge of an electron, φ_m refer to the work function of the metal gate relative to vacuum. E_{ref} refers to the reference electrode potential according to the relation:

$$E_{ref} = E_{rel} + E_{abs}$$

According to the relation (3), relative to hydrogen electrode E_{rel} refer to the potential of the reference electrode, E_{abs} is the absolute potential of the standard hydrogen electrode. All terms of equation (2) are stagnant except for the potential φ_0, which depend on the pH concentration and can be extracted with a calculation from the solution of the "EIS system". Figure 1 shows the equivalent circuit of the ISFET, with D, S, B, R being respectively the Drain (D), Source (S), Bulk (B), and the Reference electrode (R):

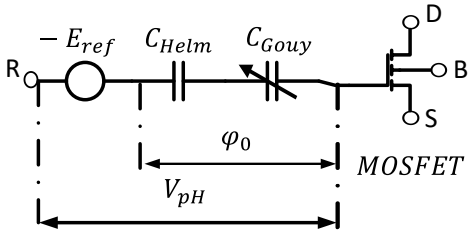

Figure. 1. Equivalent model of the ISFET sensor

The macro model of ISFET shown in figure1 treat this micro-sensor (ISFET) as two isolate stages, the first one is considered as an electronic stage since we use a MOSFET transistor, the second is the electrochemical stage which is modulated by site binding theory. We implemented this macro-model in ADS and it can be presented in figure 2 as follows:

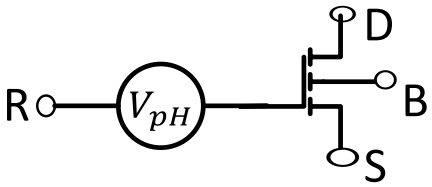

Figure. 2. The ISFET Macro-model in ADS.

where V_{pH} is potential that depends on the reference electrode and the potential of the electrolyte–insulator interface as equation (4):

$$V_{pH} = -E_r + \varphi_0 \qquad (4)$$

$$\text{With} \quad \Psi_0 = 2.3\,\frac{KT}{q}\,\frac{\beta}{\beta+1}\left(pH_{pzc} - pH\right) \qquad (5)$$

Where β is the corrective parameter for pH-ISFET which ranging between 0< β < 1. The model that we used in ADS was inspired from the reference study [15].

III. SIMULATION OF THE MACRO MODEL IN ADS

The fabrication of the ISFET was made at the physics department of research institute of micro-devices Ukraine[16]. Figure 3, illustrate the simulated macro-model and the experiment setup, in the simulation we used Advanced Design System (ADS):

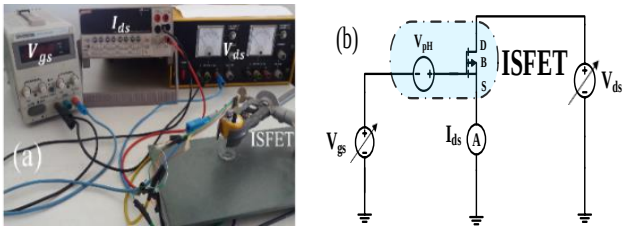

Figure 3. (a) Experiment setup, (b) ISFET macro-model.

As shown in figure 4, the extracted data from the Experimental setup were compared with the simulation of the macro model:

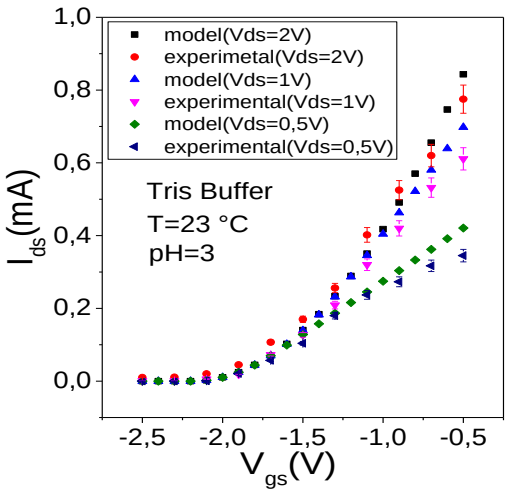

Figure 4. Macro-model versus experimental data.

By analyzing the figure above we notice that the simulated and the experiment data are in a good agreement, also, the estimated error is in order of 0.12% for $V_{ds} = 1V$ *and* $V_{gs} \in$ [-1.8 V,-0.5 V]. We used the validated macro-model in the next parts of this work.

$$\varepsilon(\%) = \sum_{i=1}^{n=8}\left(\frac{I_{ds_{exp}} - I_{ds_{model}}}{I_{ds_{exp}}}\right) \times 100 \qquad (6)$$

Furthermore, The technological parameters of the ISFET are reported in table1:

Table 1: parameters of ISFET macro model

Parameters	Values
V_{to}: Threshold Voltage (V)	-1.7
φ_0: Surface Potential (mV)	555
λ_0: Channel length (1/kV)	7.59
C_j: Junction Capacity (F/cm^2)	4.44
C_{jsw}: Junction Sidewall Capacity (pF/m)	515
T_{ox}: oxide thickness (nm)	150

Figure 5 shows the $\partial(\log(I_{ds}))/\partial V_{gs}$ variation as a function of V_{gs} for fixed values of V_{ds}=1V, we used this

method to estimate the sensitivity of the macro-model.

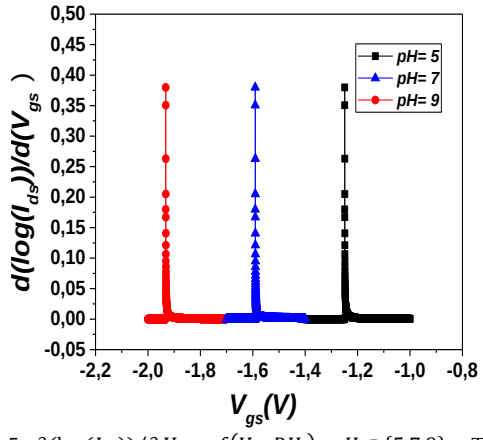

Figure5. $\partial(\log(I_{ds}))/\partial V_{gs} = f(V_{gs}, PH_i)$, $pH \in \{5,7,9\}$ at T=27°C.

Using the first derive method we extract the different values of threshold voltageV_{tI}. As consequence figure 6 shows the threshold voltage as a function of pH.

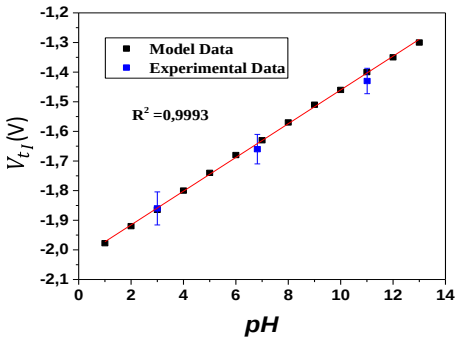

Figure 6. V_{t_I} as a function of the pH.

As shown in figure above, the estimated sensitivity of the ISFET macro-model is about of $54\,mV/pH$, also, the sensitivity found based on experiment data is in order of $51\,mV/pH$. As consequence, we conclude the ISFET macro-model is able to predict accurately the variation of chemical concentration.

IV. THE OPTIMIZED SOURCE FOLLOWER ISFET READOUT CIRCUIT

The presented circuit in figure 7 shows the proposed circuit for temperature compensation. Several researches have been report this circuit [17-19] and they report that this circuit has advantages as this configuration is grounding the reference electrode that the only one reference electrode is necessary for multiple ISFET detection. The circuit is suitable for ISFETs with unspecified characteristics because it has a wide range of operations Nevertheless, in standard CMOS technology it is difficult to integrate the Zener diode with ISFET [17-19]. With that being mentioned, here in this work we propose a solution to overcome this limitation. The diode Zener present in the [17-19] was replaced by a MOSFET transistor. As shown in figure 7 we consider the use of a single p type MOSFET with source, drain and gate connected such that there are two diodes in parallel between gate and bulk [20].

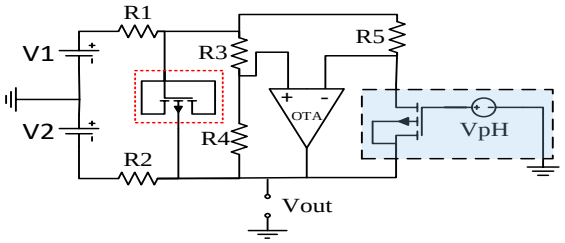

Figure 7. the presented circuit for temperature compensation

Since we work under weak inversion regime the diode zener can be replaced by a simple diode, with this configuration this has now the ability to be untegrated to ISFET based microsysteme. In deed, we propose to replace the amplifier presnt in[18, 19] by operational transconductance apmlifiere (OTA), in the nexte section we report OTA that we used in the simulation.

A. OPERATIONAL TRANSCONDUCTANCE AMPLIFIER (OTA)

In order to implant the circuit shown above in microsysteme technologie and since the optimized circuit has an important features as shown in [21]. For this reason, we choose to work with the Miller architecture for reasons such as the simplicity of the architecture and also it guarantees a low energy consumption compared to other types of OTA. Figure 8 shows OTA MILLER:

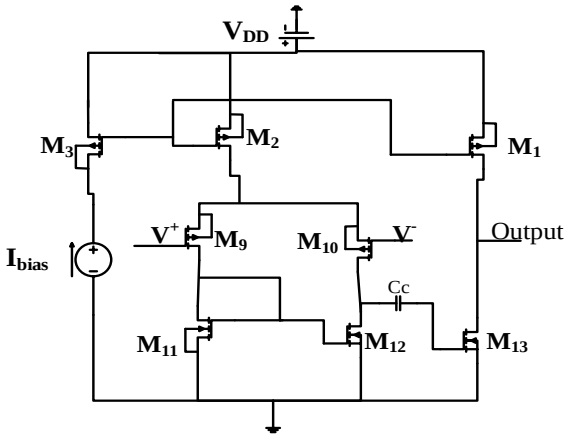

Figure 8: Two-Stage Miller OTA Amplifier [22]

In order to minimize the noise effect due to variations in the number of carriers and to fluctuations in mobility, the two P-channel M_9 and M_{10} transistors PMOS form a first stage, which is the differential stage. With this stage we can do the amplification in differential mode and reduce the common mode effect. Also, it is composed of two transistors M_{11} and M_{12} N channel (NMOS) forming an active charge (current mirror). The N-channel transistor M_{13} (NMOS) forms a second stage of the OTA which is the common source amplifier. With this stage it is possible to have amplification in differential mode. The Ibias bias current flows through the P-channel (PMOS) transistors M_1, M_2 *and* M_3 used for biasing the circuit. The I_{bias} fixed current source provides polarization. Finally, to ensure the stability of the amplifier is added the capacitance C_c (compensation capacity).

B. SIMULATION RESULTS

Figure 9 shows the improved structure of the transconductance operational amplifier. This improvement is presented by the replacement of the current source I_{bias} = 0.5 µA by a transistors

where the PMOS M4 plays the role of an active resistor and the other NMOS transistors (M5, M6, M7 and M8) form two mirrors of current. For this reason, the generation of the Ibias bias current is constant in order to supply the two-stage operational amplifier.

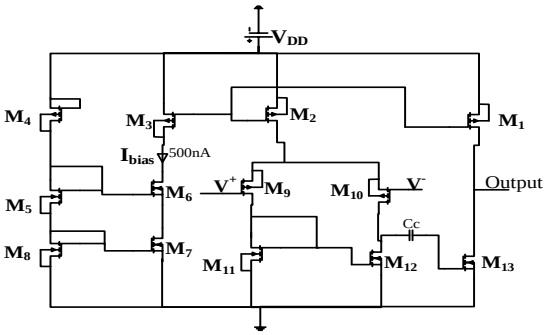

Figure 9. Enhanced Structure of the OTA Amplifier [22]

A comparative study was made to compare the performance of our operational amplifier with other op amps. From Table 2 we notice that our amplifier has competitive performance compared to other OTA especially in terms of technology and consumption.

Tableau 2. Comparative study with other works

Parameter	[23]	[24]	[25]	[26]	[27]	OTA (this work)
Technologie (µm)	0.25	0.18	0.18	0.045	0.18	0.18
Gain Av (dB)	93.365	16.3	--	--	87.74	38
Average power consumed (µW)	169.3	360	33.5	90	318	8.02
Phase margine	60.51	81.1	--	60	64.8	77.23
GBW (MHz)	5.081	115.5	41.35	--	24.8	1.22
power supply voltage (V)	--	1.2	+- 0.5	+- 0.7	+-1.8	3.3

We note from the OTA Miller show a good power consumption comparing with other work based on OTA

C. Results and Discussion

The circuit present in figure 7 was simulated under ADS simulation tools. As known in all circuit we investigate the temperature range from -20 to 150 °C, we do it the same for the circuit present in figure 7:

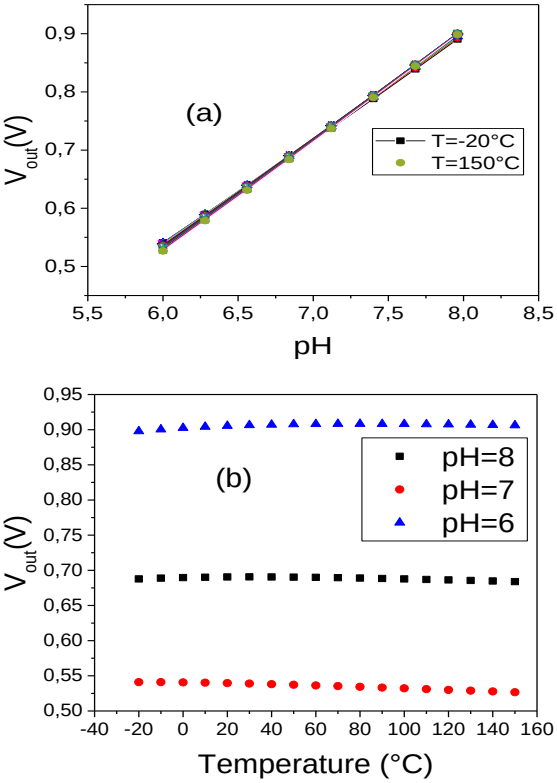

Figure 10. (a) V_{out} as a function of pH , (b) V_{out} as a function of the temperature.

As shown in figure 10 (b), the proposed circuit has a temperature drift of about 13 10^{-6} V / ° C in pH=6 for a range of -20 to 150 ° C. The components of all circuits are temperature depending. The extracted resulted from figure 10 were compared with other work in terms of temperature compensation,

Table3. Comparative study for temperature compensation

References	[28]	[29]	[30]	[31]	This work
Simulator	HSPICE	Cadence	HSPICE	ADS	ADS
Process	(AMI 1.0µm)	AMS (0.35µm)	(AMI 1.0µm)	TSMC (0.18 µm)	TSMC (0.18 µm)
Power supply	--	3.3 (V)	--	1.8(V)	1.8(V)
Power consumption	18.6 (mW)	--	--	1.8 (mW)	12 (mW)
Temperature range	[20°C, 60°C]	--	[20°C, 120°C]	[0°C, 50°C]	[-20°C, 150°C]
Temperature coefficient	28 10^{-6} (V/°C)	0.25 10^{-9} (A/°C)	23.37 10^{-6} (pH/°C)	5 10^{-6} (V/°C)	13 10^{-6} (V/°C)

As shown in table 3 the presented circuit undeniably represent an efficient and robust solution for chemical reaction sensing. Thanks to the possibilities for H+ ion detection, this system will provide great opportunities in the field of chemical sensing and Lab-on-Chip design.

V. Conclusion

In this work we had won three challenges, first one is to validate the ISFET macro-model on ADS with experimental data and we found error between the model and the experimental data about of 0.12 %. The second challenge is to propose a solution to replace the diode Zener in order to

implemented on microsystem because as noted in this work and other work that despite many advantages the diode Zener present a huge limitation for the presented circuit. And the third challenge is to switch to transistor levels for the presented circuit and a specified accent on the temperature cancellation of the ISFET. The optimized circuit shows a good temperature cancellation which is about of 13 10^{-6} V/°C for a wide temperature range from -20 °C to 150°C.

REFERENCES:

[1] X.-P. Zhang, T.-T. Wang, Z.-H. Yuan et al., "A quinoxalinone-derivated fluorescence sensor with optimized solubility for cysteine detection and biological imaging," Dyes and Pigments, vol. 171, pp. 107716, 2019/12/01/, 2019.

[2] P. Sachsenmeier, "Industry 5.0—The Relevance and Implications of Bionics and Synthetic Biology," Engineering, vol. 2, no. 2, pp. 225-229, 2016/06/01/, 2016.

[3] P. Bergveld, "Thirty years of ISFETOLOGY: What happened in the past 30 years and what may happen in the next 30 years," Sensors and Actuators B: Chemical, vol. 88, no. 1, pp. 1-20, 2003/01/01/, 2003.

[4] N. Tomari, K. Sasamoto, H. Sakai et al., "New enzymatic assays based on the combination of signal accumulation type of ion sensitive field effect transistor (SA-ISFET) with horseradish peroxidase," Analytical Biochemistry, vol. 584, pp. 113353, 2019/11/01/, 2019.

[5] M. Ortmanns, A. Buhmann, Y. Manoli et al., "Interface Circuits," Reference Module in Materials Science and Materials Engineering: Elsevier, 2016.

[6] F. Bretschneider, and J. de Weille, "Chapter 8 - Recording of Electrophysiological Signals," Introduction to Electrophysiological Methods and Instrumentation (Second Edition), F. Bretschneider and J. de Weille, eds., pp. 201-240: Academic Press, 2019.

[7] J.-C. Chou, C.-Y. Weng, and H.-M. Tsai, "Study on the temperature effects of Al2O3 gate pH-ISFET," Sensors and Actuators B: Chemical, vol. 81, no. 2, pp. 152-157, 2002/01/05/, 2002.

[8] W.-M. Munief, X. Lu, T. Teucke et al., "Reduced graphene oxide biosensor platform for the detection of NT-proBNP biomarker in its clinical range," Biosensors and Bioelectronics, vol. 126, pp. 136-142, 2019/02/01/, 2019.

[9] A. E. Kuznetsov, N. V. Komarova, E. V. Kuznetsov et al., "Integration of a field effect transistor-based aptasensor under a hydrophobic membrane for bioelectronic nose applications," Biosensors and Bioelectronics, vol. 129, pp. 29-35, 2019/03/15/, 2019.

[10] C. T. Thanh, N. H. Binh, N. Van Tu et al., "An interdigitated ISFET-type sensor based on LPCVD grown graphene for ultrasensitive detection of carbaryl," Sensors and Actuators B: Chemical, vol. 260, pp. 78-85, 2018/05/01/, 2018.

[11] G. A. J. Besselink, R. B. M. Schasfoort, and P. Bergveld, "Modification of ISFETs with a monolayer of latex beads for specific detection of proteins," Biosensors and Bioelectronics, vol. 18, no. 9, pp. 1109-1114, 2003/08/15/, 2003.

[12] M. Yuqing, G. Jianguo, and C. Jianrong, "Ion sensitive field effect transducer-based biosensors," Biotechnology Advances, vol. 21, no. 6, pp. 527-534, 2003/09/01/, 2003.

[13] P. Bergveld, W. Olthuis, A. J. Sprenkels et al., "Chapter 15 Microdialysis based lab-on-a-chip, applying a generic MEMS technology," Comprehensive Analytical Chemistry, pp. 625-663: Elsevier, 2003.

[14] S. Martinoia, G. Massobrio, and L. Lorenzelli, "Modeling ISFET microsensor and ISFET-based microsystems: a review," Sensors and Actuators B: Chemical, vol. 105, no. 1, pp. 14-27, 2005/02/14/, 2005.

[15] S. Martinoia, and G. Massobrio, "Behavioral macromodel of the ISFET in SPICE," Sensors and Actuators, B: Chemical, vol. 62, no. 3, pp. 182-189, 2000.

[16] A. M. N. Hendji, N. Jaffrezic-Renault, C. Martelet et al., "Sensitive detection of pesticides using a differential ISFET-based system with immobilized cholinesterases," Analytica Chimica Acta, vol. 281, no. 1, pp. 3-11, 1993/09/01/, 1993.

[17] F. R. G. Cruz, E. S. R. P. Montealegre, J. C. M. Aranel et al., "ISFET Bridge Type Readout Circuit with Programmable Voltage and Current." pp. 2362-2365.

[18] W.-Y. Chung, Y.-T. Lin, D. G. Pijanowska et al., "New ISFET interface circuit design with temperature compensation," Microelectronics Journal, vol. 37, no. 10, pp. 1105-1114, 2006/10/01/, 2006.

[19] M. Ali, "TopSPICE Simulations for Temperature Compensation of ISFET/MEMFET Micro- Sensor," Sensors and Transducers, 02/19, 2018.

[20] N. Moser, L. Petrou, Y. Hu et al., "An ISFET Pixel with Integrated Trapped Charge Compensation using Temperature Feedback." pp. 1-5.

[21] S. O. Cannizzaro, G. Palumbo, and S. Pennisi, "Accurate estimation of high-frequency harmonic distortion in two-stage Miller OTAs," IEE Proceedings - Circuits, Devices and Systems, vol. 152, no. 5, pp. 417-424, 2005.

[22] R. Laajimi, A novel design of low power and wide bandwidth operational transconductance amplifier using 0.35µm technology, 2013.

[23] A. C. Oliveira, D. Longaretti, L. C. Severo et al., "Design constraints correlation analysis for the automatic design of a miller OTA." pp. 72-77.

[24] M. Akbari, S. Biabanifard, S. Asadi et al., "Design and analysis of DC gain and transconductance boosted recycling folded cascode OTA," AEU - International Journal of Electronics and Communications, vol. 68, no. 11, pp. 1047-1052, 2014.

[25] A. K. Divya Garg, "SIMULATION AND ANALYSIS OF CDTA " International Journal of Advanced Research in Electronics and Communication Engineering (IJARECE), vol. 3, no. 9, pp. 3, 2014.

[26] V. Poddar, and P. Zoonubiya Ali, A Review on Low Power Designs of Operational Transconductance Amplifier with Linearity Techniques, 2015.

[27] A. Sarkar, and S. S. Panda, "Design of a power efficient, high slew rate and gain boosted improved recycling folded cascode amplifier with adaptive biasing technique," Microsystem Technologies, vol. 23, no. 9, pp. 4255-4262, 2017.

[28] S. E. Naimi, B. Hajji, I. Humenyuk et al., "Temperature influence on pH-ISFET sensor operating in weak and moderate inversion regime: Model and circuitry," Sensors and Actuators B: Chemical, vol. 202, pp. 1019-1027, 2014/10/31/, 2014.

[29] D. Ma, P. Georgiou, and C. Toumazou, "A weak inversion ISFET current mirror for differential bio-sensing." pp. 42-45.

[30] A. Harrak, and S. E. Naimi, "Design and simulation of a CMOS compatible pH-ISFET readout circuit, with low thermal sensitivity." pp. 1-6.

[31] A. Gaddour, W. Dghais, B. Hamdi et al., "Temperature Compensation Circuit for ISFET Sensor," Journal of Low Power Electronics and Applications, vol. 10, no. 1, 2020.